



Identification of typical eco-hydrological behaviours using InSAR allows landscape-scale mapping of peatland condition

Andrew V. Bradley¹, Roxane Andersen², Chris Marshall², Andrew Sowter³, David J. Large⁴

¹Department of Chemical and Environmental Engineering, Faculty of Engineering, Nottingham Geospatial Institute, Innovation Park, Jubilee Campus, Nottingham, NG7 2TU, UK

²Environmental Research Institute, University of Highlands and Islands, Castle Street, Thurso, Scotland, KW14 7JD, UK

³Terra Motion Limited, Ingenuity Centre, Innovation Park, Jubilee Campus, University of Nottingham, Nottingham. NG7 2TU, UK

⁴Department of Chemical and Environmental Engineering, Faculty of Engineering, University of Nottingham, Nottingham. NG7 2RG, UK

Correspondence to: Andrew V. Bradley (andrew.bradley1@nottingham.ac.uk)

Abstract. Better tools for rapid and reliable assessment of global peatland extent and condition are urgently needed to support action to prevent their further decline. Peatland surface motion is a response to changes in the water and gas content of a peat body regulated by the ecology and hydrology of a peatland system. Surface motion is therefore a sensitive measure of ecohydrological condition but has traditionally been impossible to measure at the landscape scale. Here we examine the potential of surface motion metrics derived from InSAR satellite radar to map peatland condition in a blanket bog landscape. We show that the timing of maximum seasonal swelling of the peat is characterized by a bimodal distribution. The first maximum is typical of steeper topographic gradients, peatland margins, degraded peatland and more often associated with ‘shrub’-dominated vegetation communities. The second maximum is typically associated with low topographic gradients often featuring pool systems, and Sphagnum dominated vegetation communities. Specific conditions associated with ‘Sphagnum’ and ‘shrub’ communities are also determined by the amplitude of swelling and average multiannual motion. Peatland restoration currently follows a re-wetting strategy, however our approach highlights that landscape setting appears to determine the optimal endpoint for restoration. Aligning expectation for restoration outcomes with landscape setting might optimise peatland stability and carbon storage. Importantly, deployment of this approach, based on surface motion dynamics, could support peatland mapping and management on a global scale.

1. Introduction

The conservation of functional peatlands and the restoration of degraded peatland, to reduce and ultimately mitigate land-use related emissions of atmospheric carbon dioxide, is now a global priority (Leifeld and Menichetti, 2018; Amelung et al., 2020; Günther et al., 2020). To support the implementation of national peatland management plans and restoration initiatives, cost-effective measures of current peatland condition and restoration progress are urgently required (Crump, 2017). Mapping peatland extent and condition has long been recognized as a huge challenge over large, remote, wet, and



often discontinuous peat forming regions where field-based surveys are impractical and expensive (Lees et al., 2018). Alternatives such as thematic mapping based on optical remote-sensing (visible and near-infra red) are increasingly used (Minasny et al., 2019), but the number of observations in regions with frequent cloud cover such as peatlands in the northern
35 latitudes and the tropics reduces the number of possible surface observations. Radio detection and ranging (Radar) that is sensitive to physical properties of the surface, provides an effective, more frequent option, given that microwave frequencies can penetrate cloud cover and return a measured signal from the ground (Minasny et al., 2019; Poggio et al., 2014). For example, using the ESA Sentinel-1 Synthetic Aperture Radar (SAR) satellites it is now possible to observe a peatland surface anywhere at high frequency (6 to 12 days) with continuous spatial coverage. When this is combined with the
40 technique of SAR Interferometry (InSAR) it allows detection of surface displacement, an indication of peatland condition, as a time-series of observations (Sowter et al., 2013).

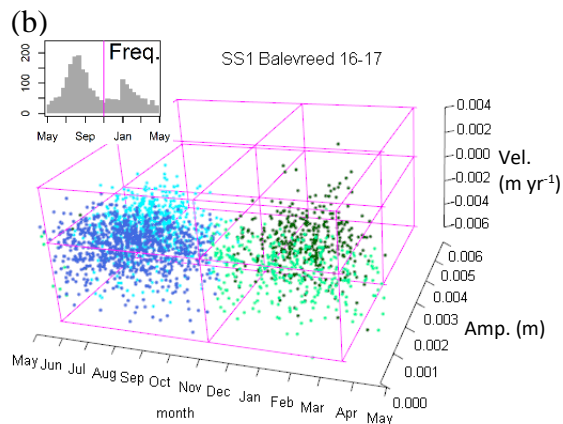
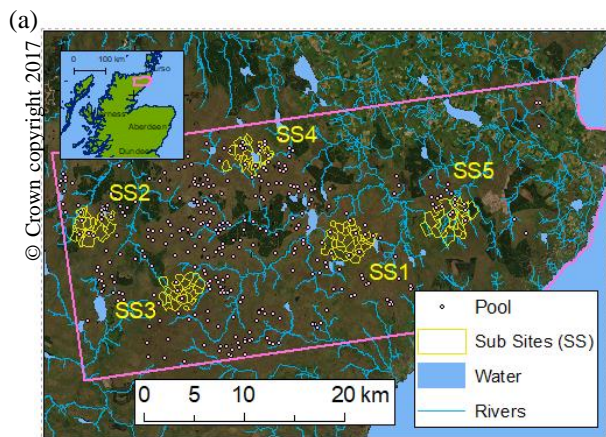
In peatlands, the rise and fall of the surface, sometimes described as ‘bog-breathing’ (Kulczynski, 1949; Baden and Eggelsmann, 1964; Mustonon and Suena, 1971; Hutchinson, 1980; Kurimo, 1983; Almendinger et al., 1986; Price, 2003; Price and Schlotzhauer, 2003) is one of the key self-regulating feedback mechanisms providing resilience and maintaining
45 function during periods of hydrological stress (Money and Wheeler, 1999; Waddington et al., 2015). This ‘surface motion’, which is a poro-elastic mechanical response to ecohydrological processes, results from the collapse and expansion of large pores in response to changes in the mass of water stored and associated stresses within the peat (Price, 2003). Mechanical deformation of the peat body and consequent surface motion can also modify the ecohydrology of a peatland via compaction, slope failure and pipe formation (Waddington et al., 2010; Waddington et al., 2015). Small-scale field
50 observations indicate that peat surface motion is influenced by changes in water level (Roulet, 1991; Price, 2003; Kennedy and Price, 2005; Fritz et al., 2008; Alshammari et al., 2020), vegetation composition (Howie and Hebda, 2018; Alshammari et al., 2020), micro-topography (Waddington et al., 2010), accumulation and upward migration of methane bubbles (Glaser, et al., 2004; Reeve et al., 2013) and land management (Kennedy and Price, 2005).

Collectively these results suggest that peatland surface motion could be a sensitive indicator of peatland function on a
55 landscape scale. So far, InSAR investigations have focused on discrete, small-scale (<1 km²) peatlands (Fiaschi et al., 2019; Tampuu et al., 2020), identifying the potential range in timing and amplitude of seasonal peatland surface motion (Alshammari et al., 2020; Alshammari et al., 2018) and its relationship to precipitation (Fiaschi et al., 2019) water level (Alshammari et al., 2020; Tampuu et al., 2020) and vegetation composition (Alshammari et al., 2020). However, peatland
60 landscapes contain a continuum of topographic, ecological, hydrological and management regimes and these small-scale studies have not captured the full spectrum of peatland conditions between degraded and near natural.

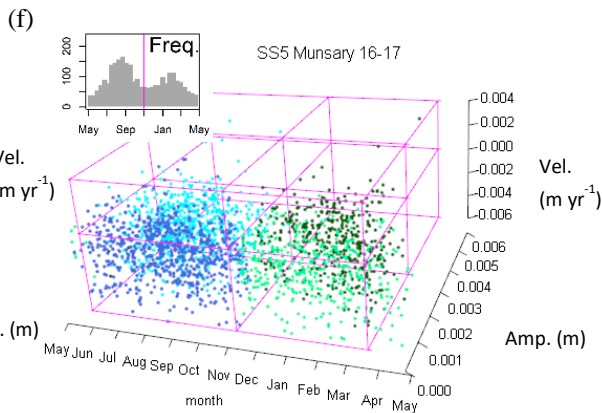
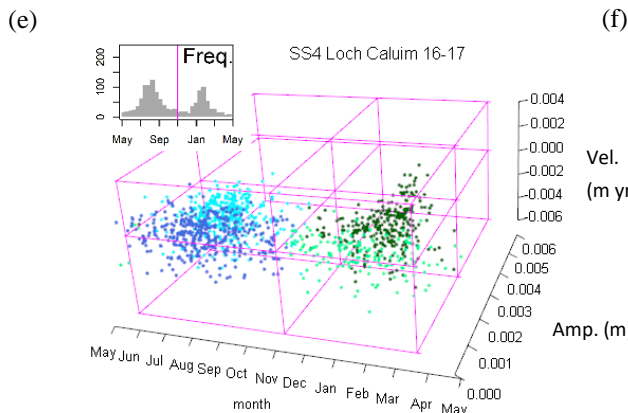
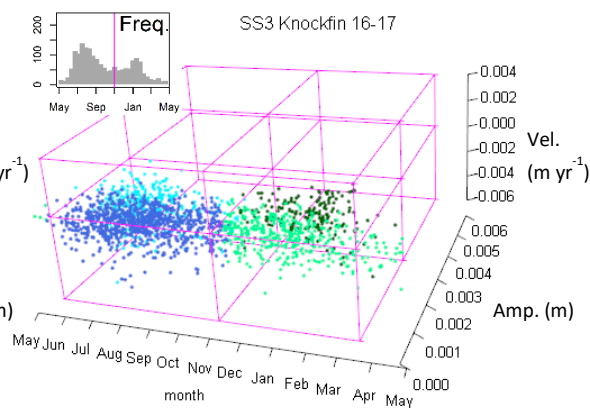
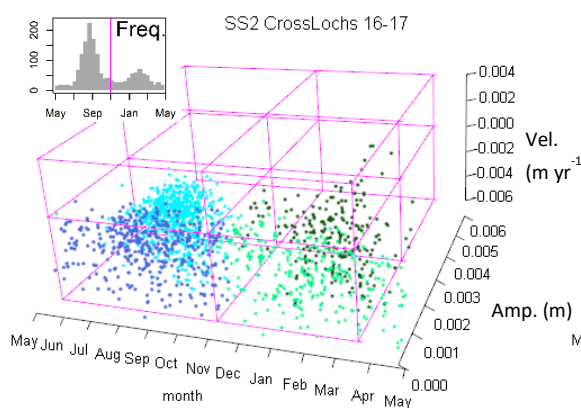
In this paper, we determine whether surface motion measured by InSAR can be used to quantify continuous changes in peatland condition over a complex peatland landscape. Using the APSIS (Advanced Pixel System using Intermittent SBAS) InSAR method formerly known as ISBAS (Sowter et al., 2013) (Materials and Methods) which is capable of generating spatially continuous measures of vertical surface motion over peatland (Sowter et al., 2013) we measure time series of



- 65 surface motion over our study site at a high spatial and temporal resolution. Specific time series metrics are then compared to independent measures of peatland condition to determine their relationship. By doing this we relate surface motion metrics to the continuum of ecohydrological conditions in this peatland landscape. Finally, we demonstrate how surface motion metrics can be used to map the ecohydrology of a peatland system. By doing so we illustrate how our new approach could be applied to monitoring the response of global peatlands to restoration, management, and climate change.
- 70 Our chosen study site is 930 km² of undulating blanket bog, ranging from 50 to 600 m.a.s.l in the Flow Country, Northern Scotland (Andersen et al., 2018; Fig. 1a). In the past, management has involved artificial drainage of the driest peatlands, targeted for subsidized agricultural improvement and later afforestation programs (Sloan et al., 2018). More recently, wetter near natural areas have been designated for conservation (Lindsay et al., 1988), and previously forested and drained areas are now undergoing restoration. Some areas are actively eroding, particularly at the highest altitudes (Hancock et al., 2018). This
- 75 complex mosaic of near-natural and modified peatland conditions within this study site makes it particularly suited to the use of InSAR mapping of peatland condition.



(c) ESRI World Imagery (d)





80 **Figure 1: Study location, Sub Sites (SS) and the surface motion metrics plots calculated from InSAR detected annual motion**
between May 10th 2016 to May 9th 2017. (a) The study location (inset) and study area, outlined, in the Flow Country, Northern
Scotland. Forested areas are dark green, with the main river network shown. Plots for, (b) SS1 Balavreed, (c) SS2 Cross Lochs, (d)
85 SS3 Knockfin Heights, (e) SS4 Loch Caluim, (f) SS5 Munsary. Axis: x, time (months); y, amplitude (amp.: m), z, velocity (vel.: m
yr⁻¹) with inset frequency (Freq.) histograms of peak timing in each of the sub sites. For velocity, +ve is upward and -ve is
downward motion of the surface. Histograms of peak timing at all sites display a bimodal distribution and the points on the scatter
plots are colored to illustrate their relative position. Pale green and dark blue points are towards the front (low amplitude) and
dark green and pale blue points are towards the back (high amplitude). Image sources for (a): ERSI World Imagery, sources Esri,
90 DigitalGlobe, GeoEye, i-cubed, USDA FSA, USGS, AEX, Getmapping, Aerogrid, IGN, IGP, swisstopo, and the GIS User
Community, © Crown copyright 2017. Distributed under the Open Government Licence (OGL). Ordnance Survey (Digimap
Licence).

2 Materials and Methods

2.1 Data and time series processing

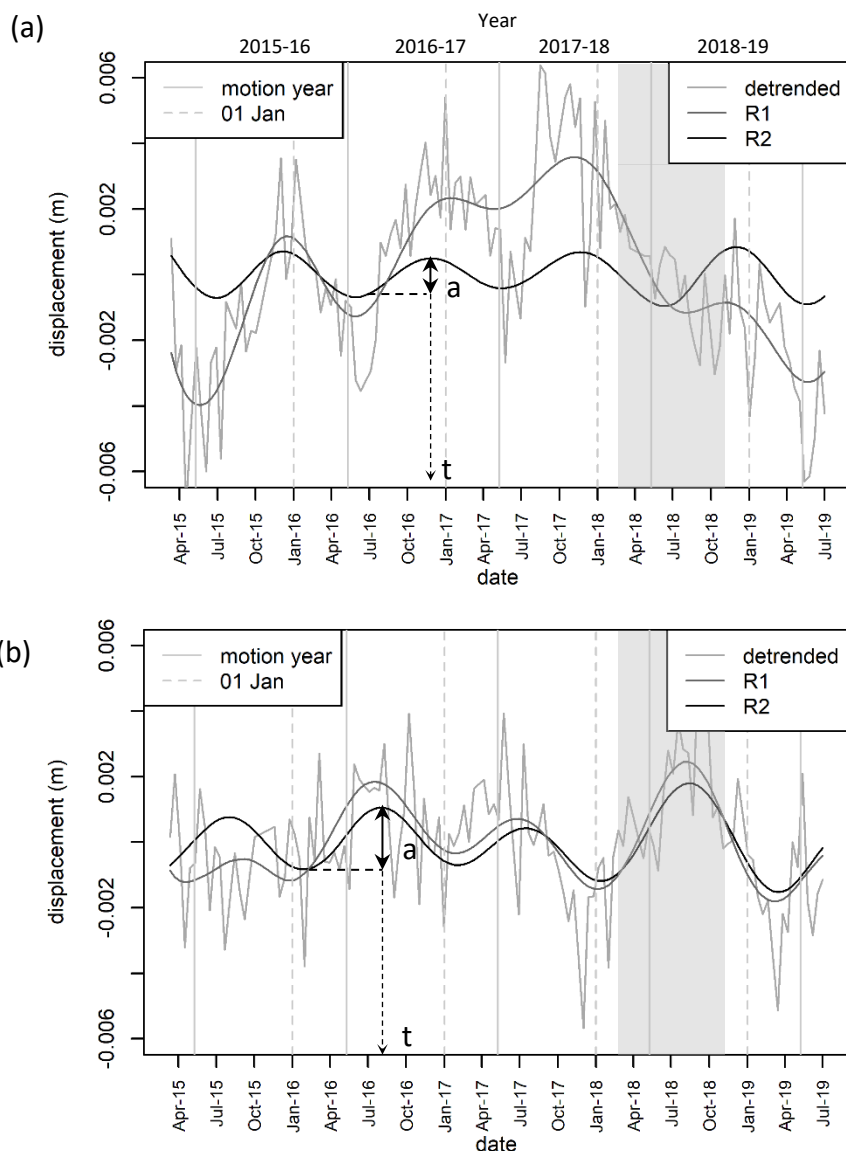
To calculate the surface motion, we used 410 Sentinel-1A and -1B synthetic aperture radar images (Descending Orbit 125)
gathered every 6 to 12 days between 12/03/2015 and 01/06/2019 from the European Space Agency Copernicus Open Access
95 Hub (<https://scihub.copernicus.eu>). Satellite interferometry was applied using these images with the Advanced Pixel System
using Intermittent SBAS (APSiS) technique. This technique, which was formerly known as the intermittent small baseline
subset (ISBAS), is an advanced DInSAR technique (Sowter et al., 2013). The APSiS technique contains an adapted version
of the established SBAS DInSAR time series algorithm (Bateson et al., 2015; Cigna and Sowter, 2017). It was designed to
improve the density and spatial distribution of survey points to return measurements in vegetated areas, where DInSAR
100 processing algorithms habitually struggle due to incoherence (Osmanoğlu et al., 2016; Gong et al., 2016).

The APSiS algorithm was implemented using Terra Motion Limited's in-house Punnet software, which covers all aspects of
processing from the co-registration of SLC (Single Look Complex) data to the generation of time series (54). Maximum
horizontal baseline was restricted to 250m with maximum temporal separation of 1 year using a coherence threshold of 0.25
and point threshold of 360. Motion was measured relative to a stable reference point at Wick Airport (58.4533° N, 3.0879°
105 W). Phase unwrapping was implemented using an in-house implementation of the SNAPHU algorithm (55). Using APSiS,
two products were produced for each georeferenced pixel location at approximately 80 by 90 m resolution. A motion time
series of multiannual average line-of-sight velocity (m yr⁻¹), and the time series of surface motion from which we are able to
detect the seasonal expansion and contraction (or bog breathing) as annual oscillations in relative height (L. Alshammari, et
al., 2018).

110 Each motion time series was processed as follows, to quantify the specific peatland surface motion metrics. Firstly, using
the R programming environment (R Core Team, 2013), the time series was sub-sampled into equal time intervals of 12 days,
to match the longest overpass interval of Sentinel-1 images since Sentinel 1B, which reduces overpass times to 6 days, was
not operational until 2016. Outliers were re-estimated using the R 'tsclean' function (Box and Cox, 1964), from R package
'Forecast' (R. Hyndman et al., 2020). Gaps were filled with a linear interpolation using the R 'approx' function (Becker et
115 al., 1988) from R 'stats' package (R Core Team, 2020) after 'spline' methods were found to produce contradictory results



when considering adjacent time series across the largest gaps. The ‘detrend’ R function aligned and reset each time series around zero by subtracting the mean. Secondly, MSSA using the SSA-MTM toolkit (Ghil et al., 2002; SPECTRA, 2021) was applied to extract the cyclical seasonal trend from the 4-year 5-month time series. Covariance was calculated after channel reduction with Principal Component Analysis (PCA). Using a moving window of 12 months, long enough to capture annual cycles, we calculated the first 10 PCA channels and 20 Empirical Orthogonal Functions (EOFs) to identify the seasonal cycles in the time series. In the first instance, surface motion time series were reconstructed using EOFs 1 - 6 (Fig. 2). This reconstruction captured the seasonal cycles but also included longer-term climate trends, notably three wetter years leading to the 2018 European wide drought (Buras et al., 2020). This climate trend causes merging and shouldering of peaks that compromised the detection of the seasonal cycles, particularly in the west of the study area, where it is wetter. To overcome this difficulty, we used a surface motion time series reconstruction using EOFs 5 and 6 (Fig. 2; Supplement 1.1 Fig. S1) which extracted only the seasonal cycles. As the 2018 drought caused severe and widespread subsidence it subdued the multiannual average velocity. This was mitigated by recalculating multiannual average velocity for three complete motion cycles (March 2015 to March 2018) prior to the 2018 drought.



130 **Figure 2: Examples of surface motion time series and the metric definitions for (a) wet bog and (b) a drier bog, calculated from**
 Sentinel-1 APIS InSAR time series data between 12 March 2015 and 01 July 2019. The initial mean detrended time series (grey),
 and MSSA Reconstructions (R) retaining the local climate trend (R1, mid grey, a combination of empirical orthogonal functions 1
 - 6) and annual seasonal cycles (R2, dark grey a combination of empirical orthogonal functions 5 and 6) are shown. The two
 surface motion metrics used in the analysis are, peak amplitude timing (dotted line, t), and amplitude (solid line, a) shown for the
 135 annual surface motion year May 10th 2016 to May 09th 2017. A third surface motion metric, multiannual average velocity is not
 defined here as it is part of the InSAR data processing (Materials and Methods). This asynchronous timing of peaks between (a)
 and (b) forms a bimodal distribution in the peak amplitude timing of the peatland landscape. The drought event of 2018 is
 indicated by the shaded column (Buras et al., 2020) and can be seen to influence the local climate trend in the wet bog (a). For
 MSSA details see Materials and Methods.



140 Peak timing and amplitude of the seasonal cycles were extracted (Fig. 2) for individual years, using the R ‘pracma’ peak-find
function (R Core Team, 2013). For measurement purposes, the start of the year was set to May 10th to avoid splitting the
period in which the seasonal peak was likely to be detected. The measurement was not performed on the first and last years
in the time series (2014 to 2015 and 2018 to 2019) as surface motion cycles are truncated preventing the accurate calculation
of amplitude and peak timing. Surface motion time series were also tested to find multiple peaks per annum or years where
145 detection was not discernable, and these pixels were classed as having Irregular cycles (IRR). Irregular time series made up
8.4% of the data set and are commonly associated with water courses and damaged bog (including agriculture and forested
areas) (Fig. 4). Exclusion of these irregular time series from the surface metrics plot (Fig. 1) does not affect our conclusions.

2.2 Ecohydrology of study area and sub-sites

The Flow Country peatlands exist in a range of topographic, hydrological and management settings, leading to a range of
150 different conditions e.g., from highly eroded to relatively intact peatlands, superimposed by activities such as forestry,
drainage, and grazing across an undulating landscape. We predicted that the values of the three motion properties would
spatially vary from one place to another showing as small variations on the shape of the 3-axis cluster plot as the values in
amplitude, velocity, and timing subtly shift from place to place. To demonstrate this, the five areas of peatland covering a
range of conditions, roughly 10-15 km², defined as the sub-sites, were chosen based on local expert field knowledge and are
155 summarized in Table 1.

Table 1: Details of the five subsites (SS), which are all currently designated as Site of Special Scientific Interest (SSSI), Special Protection Areas (SPA) and Special Areas of Conservation (SAC).



SS	1	2	3	4	5
Name	Balavreed	Cross Lochs	Knockfin	Loch Caluim	Munsary
Location	58.38N -3.50E	58.39N -3.94E	58.32N -3.80E	58.44N -3.68E	58.39N -3.35E
Altitude (m.a.s.l)	~180	~180	~360	~120	~100
Topography	Watershed, gently undulating with pool systems	Flat pool systems with steep slopes into a valley	Eroding on upland ridge with ephemeral pools, and hags (wind eroded peat islands),	Gently sloping into central loch	Gently undulating area incised by small steams
General condition	Near-natural	Near- natural, drier peat	Eroding peat	Near- natural	Near natural surrounded by agricultural conversion and forestry
Current management	Low level sheep and deer grazing, conservation management agreement	Low to medium grazing by deer. Includes restoration (forest-to-bog and drain blocking) areas. Conservation management as part of Forsinard	Deer grazing, Forestry to the north and drainage to the East. Conservation management as part of FFNNR	Low level sheep and deer grazing, under conservation management agreement with FFNNR	Intense drainage for agriculture and grazing surrounded by forestry and forestry to bog to east and South. Part of the site under conservation management by Plantlife Scotland.



Flows
 National
 Nature
 Reserve
 (FFNRR)

History	Evidence of damage from historic burning and drainage (hill drains) in places alongside natural drainage lines.	Surrounded by restoration areas (forest-to-bog undertaken in 2006) and standing forestry on deep peat. Wildfire in 1981	The surrounding areas have been drained and burnt in the past	Some historic drainage and peat cutting. The area was also historically used for cattle grazing and is part of an old drove road.	Historic drain blocked with plastic piling, Historic drainage and burning
----------------	---	---	---	---	---

160 **2.3 Ecohydrological classification of the sub-sites**

To identify the links between surface motion and the ecohydrology, the training bed of the sub-sites SS1 to SS5 were divided manually using Google Earth images, into 130 smaller polygons (most between 0.3 – 0.6 km²). To construct the polygons, one of the authors without specialist peatland knowledge used distinct contrasts where there were changes in the landscape structure, e.g. pool systems, visible drainage, vegetation reflectance and, evidence of land use management, e.g. fields and drainage as well as consistency in peak timing. In addition to the sub-site polygons, 125 random points were selected across the whole study area using the ESRI ArcMap “random point” tool. The immediate area close to the point was assessed for features in the landscape, (e.g., topographic setting, natural drainage, evidence of drainage ditches and where these features would influence hydrology, forests, restoration, management and the likely range, consistency or inconsistency in peak timing) and used to draw polygon boundaries to include this variation (most between 0.2 – 0.5 km²). While the sub-sites included the continuum of conditions and features adjacent to each other, the random polygons captured the ecohydrological state across the whole study area and avoided sample bias from the sub-sites. Measures of topography (average altitude, slope and aspect for all points in the polygon) were calculated from the Shuttle Radar Topography Mission Digital Elevation Model (Jarvis et al., 2008) for each polygon (Supplement 1.3).



The full set of polygons (sub-sites and random) was then passed to one of the authors with specialist peatland knowledge for a “blind” (i.e., without prior knowledge of or information about InSAR metrics) eco-hydrological classification. For each polygon, the cover of Plant Functional Types (PFTs); Sphagnum, other mosses, shrub, sedges, grasses, rushes, and conifer trees) and the presence of hydrological features (pools, streams, drains, erosion gullies, slope), were recorded using a semi-quantitative scale, (0 = not present or scarce, 1 = present, 2 = co-dominant, 3 = dominant). Current management (conservation, drainage for agriculture and peat cutting, forestry, restoration by forest-to-bog, and restoration by drain blocking) and historical management (e.g., burning, land-use conversion including wind-farm construction, restoration), was also documented for each polygon. This was achieved through a combination of existing data, field visits, local knowledge, 1:50 000 UK Ordnance Survey maps, NatureScot National Vegetation Classification maps (64), and Google Earth imagery. The author responsible for classification visited and surveyed all the sub-site polygons and 86 of the random polygons (85% of the polygons).

Using the semi quantitative scores, the vegetation and hydrology polygon attributes were clustered by similarity using a Hierarchical Cluster Analysis (HCA; Supplement 1.4, Fig. S3) to identify similar combinations of vegetation. To avoid an overly split hierarchical tree with only one or two members per cluster requiring complex explanation, it was deemed more informative to analyze the vegetation, hydrology and the topography category’s separate from each other. For the vegetation, once the classes had been clustered, the average score for each category in the cluster was ranked with the top three PFTs used to characterize the plant functional group composition. Absence of a PFT was also noted (Tables S1-S4). For data visualization, clusters were grouped based on the dominant PFT, resulting in five groups: Sphagnum, Shrub, Grass, Bare peat (where Low or Absent vegetation was dominant) and Forestry. Very few clusters had were dominated by rushes (R) and all those had shrub as a co-dominant vegetation, so they were incorporated into the Shrub group. While sedges (Sg) were co-dominant in both Sphagnum and mostly shrub clusters, they were not the dominant PFT in any clusters and therefore did not form a separate group. These categories are used and expanded in the captions of Table 2.

Table 2: Percentage proportion of clusters derived from Hierarchical Cluster Analysis based on plant functional types (PFTs) represented in the polygons of the five sub-sites and the random polygons. Clusters are defined by the dominant (first) and co-dominant (subsequent) PFTs. PFT notations: Sp = Sphagnum, S = Shrub, Sg = Sedges, M = Moss, G = Grasses, R= Rushes, F= Forest, LoA = Low or absent vegetation (Brash, bare peat following tree felling or restoration activities etc.). PFT in brackets denotes a notable presence. n=number of polygons. For data visualization, clusters were grouped based on the dominant PFTs in five groups: Sphagnum, Shrub, Grass, Bare peat and Forestry. Clusters dominated by Rushes (R) were incorporated in the shrub group for data visualization given their low number and shrub co-dominance. The group’s Bare peat and Forestry were kept despite low numbers, as their vegetation is associated to specific management intervention.

205

Group	Sub-sites	SS1	SS2	SS3	SS4	SS5	Random	All
-------	-----------	-----	-----	-----	-----	-----	--------	-----



Name	Clusters	%					Clusters	%
SPH	Sp,S,Sg	37.9	29.6	0	45.5	19.2	Sp,Sg,S	28
SHRUB	S,Sg,Sp(G)	17.2	14.8	0	13.6	0	S,Sg,M/ Sp	28
	S,Sg,R	10.3	48.1	3.8	4.5	34.6	S,Sg,G,M	8
	S,Sg,M	20.7	0	69.2	9.1	0	S,G,R	8
	S,Sg,M(G)	3.4	0	23.1	18.2	0		
	R,S	0	0	0	0	3.8	R,Sg,S	4
GRASS	G,S,R	10.3	3.7	0	4.5	11.5	G,R,S, nSp,nM	8
	G,R	0	0	0	4.5	11.5	G,S,R	1.6
BARE	LoA	0	0	0	0	7.7	LoA	4
FOR	F	0	3.7	3.8	0	3.8	F	9.6
	<i>n=</i>	26	27	26	22	29	<i>n=</i>	125

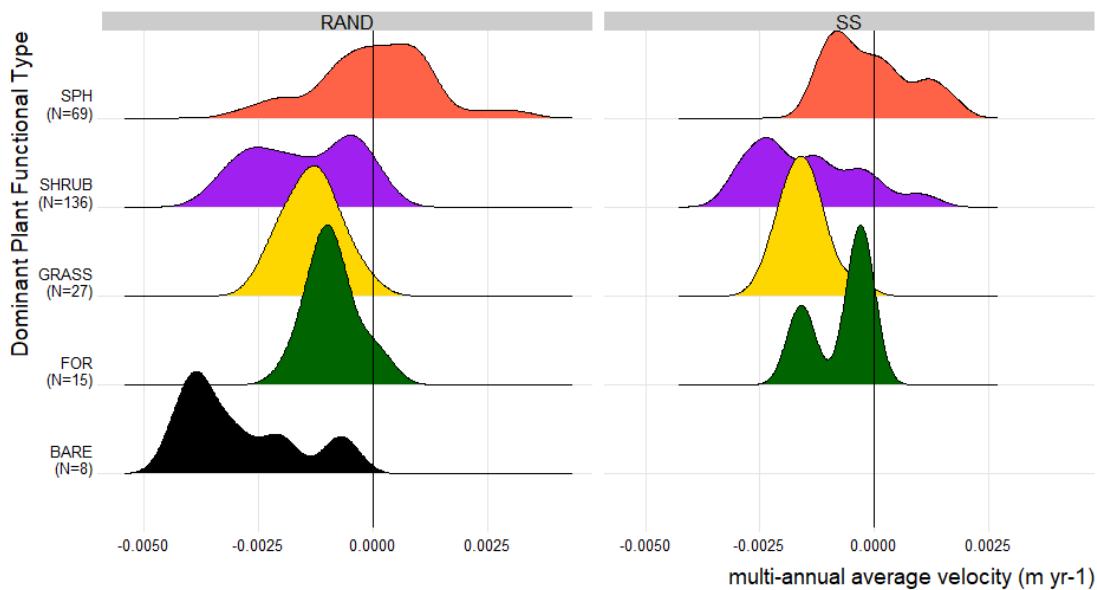
We also categorized topography into 1 = low, 2 = med and 3 = high, and split slope face direction into four quadrants and passed the data through an HCA. Except for the eroded SS3 site, altitude and aspect did not show any meaningful cluster groups and played no further part in the analysis. The lack of topographic relationships are largely due to the gentle relief of the Flow Country that has few sheltered slopes and valleys. Instead, we used average gradient (degrees) in the polygon and found a natural breakpoint at 1.5 degrees that split the dataset equally between FLAT (< 1.5 degrees) and SLOPE (>1.5 degrees), with most pools with Sphagnum found in FLAT (Fig. 3a).

(a)

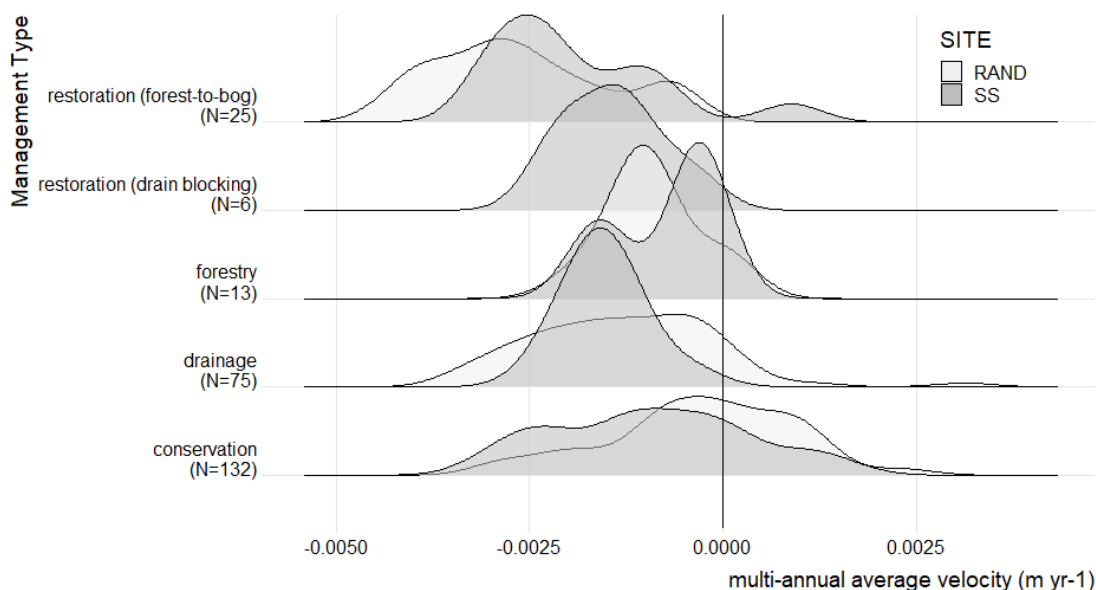


215

(b)



(c)



220 (d)



225

Figure 3: Polygon summaries with respect to dominant plant functional clusters, management groups, topography and the three motion metrics. (a) Distribution of median polygon peak timing over time (month) for dominant plant functional clusters for polygons with pools, streams or other hydrological feature (e.g. drains, erosion gullies, peat cutting, or no apparent features) in either FLAT (gradient < 1.5°) or SLOPE (gradient > 1.5°) topographic setting. Plant functional clusters: BARE = bare peat, FOR = conifer plantation, GRASS = grass-dominated communities, typically *Molinia caerulea*, SHRUB = shrub dominated communities, typically *Calluna vulgaris* and/or *Erica tetralix*, SPH = Sphagnum dominated communities. Sedges, rushes and other mosses are also present, often as co-dominant species in both SPH and SHRUB communities (see Table 2). Months are numbered



230 from May (05) through to the following April (04). (b) Joy plots showing the variation in multiannual velocity for each plant functional group, polygon type (RAND= Random, SS=sub-site) and topography. (c) Joy plots of multiannual average velocity for different management groups (restoration, forestry, drainage, conservation) by polygon type (RAND, SS). (d) The timing of and relative amplitude for three consecutive years (2015-2018) with respect to slope gradient (degrees), dominant plant functional clusters (GRASS, SHRUB and SPH), and by polygon type (RAND, SS).

235 Summary statistics of the three surface motion metrics were made for each polygon. Although one side of the binomial distribution usually dominated, the median score of each polygon was used over the mean. This is because the transitional nature of the environment (i.e. a wet peat center has drier edges with slightly different vegetation composition), where polygon edges may consist of some pixels from the opposite side of the bimodal distribution (Fig. 1b-f) causing a slight skew in their distributions. The use of the median score was found to reduce these effects for Fig. 3d.

2.4 Mapping the state of the peatland system

240 To test whether the metrics of peak timing, amplitude and multiannual velocity can be used to map and predict peatland condition we classified the position of pixels within the surface motion metrics plot. The classification was based on the Euclidian distance from what restoration practitioners would consider a reference point corresponding to a good condition 'wet' Sphagnum peat. This is characterized by high amplitude (e.g., 0.008 m), a positive multiannual velocity (e.g., 0.006 m yr⁻¹), and the most frequent peak timing of the 'wet' Sphagnum dominated condition (e.g., February) within a plot of amplitude vs. peak timing vs. multiannual velocity for the entire study area. The actual reference point was selected by
245 stepping down through the percentiles of the metrics distributions until the case with, the most frequent timing, highest positive velocity and highest amplitude was identified. It would also be possible to integrate field observations and choose the reference point values from specific pixel(s) if a particular condition was to be investigated. Data for each pixel were paired with the reference point and the Euclidian distance in 3-dimensional (Cartesian) space was calculated. If the paired
250 pixel was in the 'dry' shrub side of bimodal distribution, the Euclidian distance was mapped as a 'V' shaped path via zero velocity and zero amplitude at the mid date, 10th November, between the 'wet' Sphagnum and 'dry' shrub conditions. Prior to calculation, the positions of the outer portions of the 'wet' and 'dry' distributions were adjusted. This is because if the paired point is earlier than (left of) the dry peak and later than (right of) the wet peak the difference between the peak timing and the origin would be incorrectly estimated. To mitigate this, these cases were folded inwards along the axis of the peak of
255 their distributions (effectively turning the upturned 'W' shape of the bimodal distribution into an 'M' shape). Using the natural breaks (Jenks) classification as a guide in ESRI ArcGIS, thresholds were used to map 'wet' Sphagnum dominated, 'dry' shrub dominated and the thin/modified peat classes across the whole study site to produce an ecohydrological map (Fig. 4d).

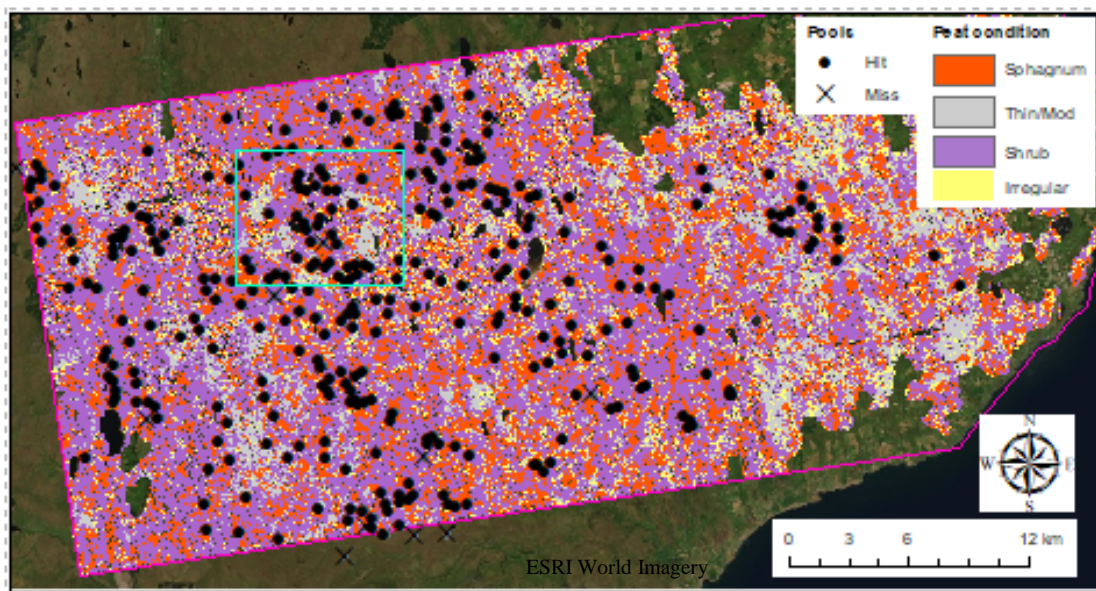
260 To verify the predictive accuracy of the ecohydrological map we remotely identified the central locations of all the pool systems (328 in total), within the study area using Google Earth images, and compared if these points corresponded to the Sphagnum 'wet' condition. To capture the wider complex morphology, varying geometries (and sometimes variable condition) of a full pool system (Lindsay, 2016), a search area of 150m (using the buffer function in ESRI ArcMap) was then



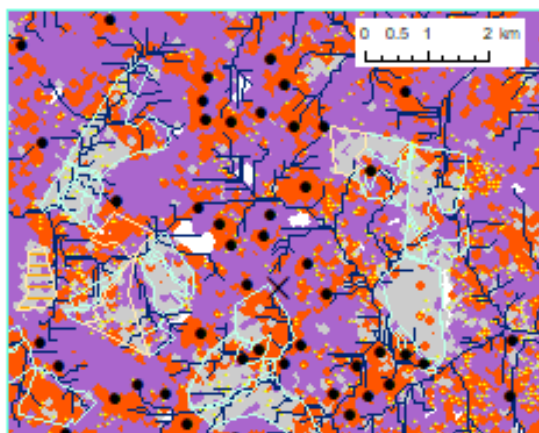
calculated. This buffer area contained at least 3 by 3 pixels of the ecohydrological map. We then calculated the percentage of Sphagnum ‘wet’ pixels in the buffer. Pixels classed as irregular were not included in the count (Table S5).



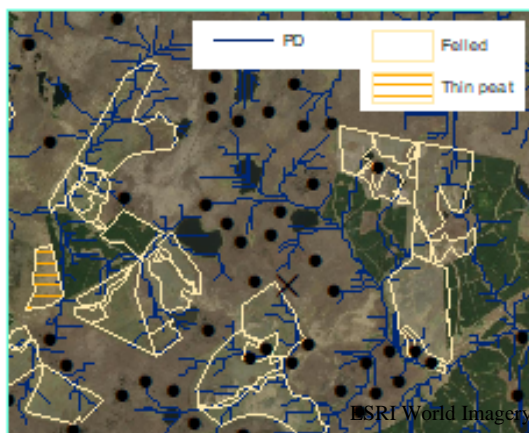
(a)



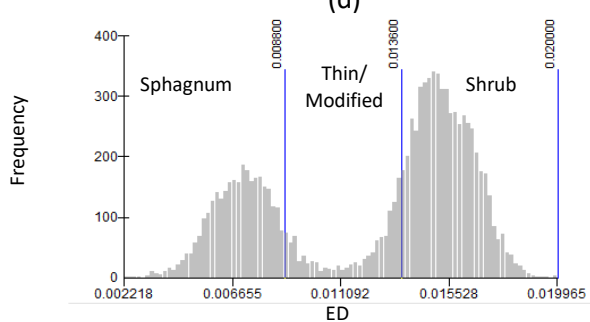
(b)



(c)



(d)





270 **Figure 4: The classification of peatland condition, with respect to the location of pool systems, and areas of forest-to-bog restoration in the study area. (a) Classified map based on the Euclidian distance (in 3-dimensional Cartesian space) from the position of a ‘wet’ Sphagnum endmember of each point in the plot of peak timing, amplitude and multiannual velocity for the period June 2016 to May 2017. Three peat classifications are indicated, Sphagnum, Thin/modified, and Shrub. Pixels that could not be classified due to an absence of distinct seasonal oscillation are classified as irregular. The classified area (approx. 930 km²) was delineated using peat soils from the National Soil Map of Scotland (JHI, 2021). Points in pool systems that have been correctly classified are shown as a “hit” and those incorrectly classified as a “miss”. (b) A detailed view of the classified area highlighted within (a) illustrating the relationship with potential drainage (PD), determined from a DEM, areas of thin peat (hatched), and peat areas at various stages of forest to bog restoration (outlined) ranging from recently felled (thin/modified class) to almost fully restored via rewetting (Sphagnum class). (c) A true colour satellite image of area, (b). Some of these restoration areas now have conditions of wet peat. (d) Frequency distribution of Euclidian distance, and the thresholds used to highlight the three peat conditions, Sphagnum dominated, Thin/modified and Shrub dominated. Images sourced via ESRI ArcMap in 2021. The variability seen within the felled forest blocks reflects variable degree of recovery associated with varying starting conditions, time since initiation of restoration (ranging from 0 to >15 years), landscape position and technique of the intervention. Image source for (a) and (c) ESRI World Imagery: Esri, DigitalGlobe, GeoEye, i-cubed, USDA FSA, USGS, AEX, Getmapping, Aerogrid, IGN, IGP, swisstopo, and the GIS User Community.**

275

280

3 Results

3.1 Surface motion in blanket peatland

InSAR surface motion time series and long-term average motion were generated for the period March 12th 2015 to July 1st 285 2019. In the timeseries, the height of the surface was calculated relative to its first point and was determined every 6 days at pixel resolution 90 x 80 m across the study site. Seasonal cycles, subsiding during the summer and rising in the winter were observed in time series from the majority of pixels. From this, we defined a motion year beginning at the least active period in May and thus avoided dissection of the peaks in the distribution. We then focused our analysis on the period May 10th 2015 to May 9th 2018 to minimize uncertainties from a drought in mid to late 2018 (Buras et al., 2020), and illustrate data 290 for the central year, 2016 to 2017, where the buildup and continuation of adjacent years is complete.

Multichannel Singular Spectrum Analysis (MSSA) was applied to the dataset to isolate this cyclical, annual seasonal component of the time series (Fig. 2) and the following three surface motion metrics used to represent the condition of the peatland within each pixel. Metric one, the timing (date) of the annual peak in the seasonal cycle within 12 months from mid-May (Fig. 2). This has been shown to relate to peatland ecohydrology (L. Alshammari, et al., 2020; Tampuu et al., 295 2020). Metric two, the annual maximum amplitude (m) in surface motion measured from the previous seasonal minimum (Fig. 2). This is an indicator of the elastic response of the peat to changes in water storage (Roulet, 1991; Waddington et al., 2010). Metric three, the multiannual average vertical velocity (m yr⁻¹) of the peatland surface. This is a measure of peatland growth (positive value) or subsidence (negative value) calculated over a fixed section of the time series (Sowter et al., 2013; Materials and Methods).

300 To understand the variation and distribution of our metrics across a spectrum of peatland conditions, we plotted them over five well-documented 10 to 15 km² sub-sites within the study area. These sub-sites span a range of landscape settings and ecohydrological conditions, from a gently undulating low-lying watershed with well-developed pool systems to actively eroding high plateau (Table 1, Fig. 1a). Plots of the metrics from the sub-sites all show features of a bimodal data



305 distribution with respect to annual peak timing (Fig. 1b-f). The bimodal distribution peaks fall between August to October
and December to February. Each sub-site shows a variation in the range of amplitude and velocity (Fig. 1b-f), reflecting the
diversity of peatland conditions sampled across the landscape.

3.2 Relationship between surface motion and eco-hydrology

To understand the link between the surface motion metrics and peatland condition, we divided the sub-sites into 130
polygons (0.2 to 0.6 km²) in which metrics were aggregated. Additionally, 125 similarly sized individual polygons were
310 generated, randomly distributed across the whole study area. This size was practical for reliable field and map-based
validation and meaningful for capturing key features of the landscape (e.g., pool systems, forestry or restoration block,
stream and banks). Dominant plant functional types (Sphagnum, sedges, shrub, grass, bare peat, forestry), hydrological
features (pools, erosion gullies, streams, drainage ditches), topographic setting (slope, elevation) was recorded for each
polygon and used for eco-hydrological classification (Materials and Methods; SI Appendix).

315 A hierarchical clustering approach (HCA; Fig. S3) revealed ecological groups relating to dominant plant functional types
comparable between sub-sites and random polygons (Table 2) as well as hydrological groups separating polygons with pool
systems and those with streams from all other polygons. Comparison of the HCA based classifications and topographic
information (slope) to the surface motion metrics enables consistent relationships to be determined for sub-sites and random
sites, as follows. First, shifts in the polygon monthly peak timing distributions relate to a combination of topography,
320 hydrology, and plant functional group (Fig. 3a). Within the hydrological class POOL, polygons with topographic gradients
greater than 1.5°(RAND SLOPE, SS SLOPE), have their highest monthly frequencies earlier in September and or October
than polygons on flatter ground with topographic gradients less than 1.5°(FLAT), which tend to be November, January and
February. The steeper gradients, RAND SLOPE, SS SLOPE, tend to be associated with SHRUB and GRASS dominated
vegetation types with low frequencies of Sphagnum dominated polygons (SPH). Polygons with POOL as the dominant
325 hydrological feature tend to have their highest frequencies from October onwards, later than polygons with STREAM or
OTHER, independent of being FLAT or SLOPE. Sphagnum-dominated polygons (SPH) are almost exclusively associated
with POOLS and flat ground (RAND FLAT, SS FLAT), and tend to have their highest monthly frequencies later in the year
(November to February) than the other hydrological and topographical situations which are mainly SHRUB dominated
polygons as well as the other PFTs, such as GRASS, FOR and BARE.

330 Second, the most positive values of multiannual average velocity were almost entirely dominated by Sphagnum (SPH, Fig.
3b). Polygons with plant functional types typically associated with natural or man-made drainage (SHRUB), disturbance
(forestry (FOR) and bare peat (BARE) or thin, degraded peat (GRASS) consistently displayed negative long-term
(multiannual) average velocities regardless of topographical setting. Sites in which grass or forestry dominate tend to have a
more intermediate multiannual average velocity than either SHRUB or Sphagnum (SPH) dominant polygons. Where bare
335 peat is dominant, the most negative velocities occur.



Third, when multiannual average velocities are compared across different management classes (Fig. 3c), the least negative values are observed under conservation management and most negative values are associated with forest-to-bog management, a restoration approach that typically involves compaction from heavy machinery during the removal of conifer stands, followed by drain blocking and surface re-profiling. This restoration class shows a broader distribution in long term
340 multiannual average velocity than other management classes, reflecting variable degree of recovery associated with differing starting condition, time since initiation (ranging from 0 to >15 years) and techniques used in the intervention.

The factors controlling amplitude can be deduced from amplitude and peak timing plots for the three most dominant PFT clusters (SHRUB, SPH and GRASS) across three surface motion years (Fig. 3d). These graphs all show a strong linear relationship between timing (day of year) and amplitude with higher amplitudes occurring later in each surface motion year.
345 Steeper slopes are more likely to have lower amplitudes that peak earlier in each surface motion year. Shallower slopes are more likely to have higher amplitudes and peak later in the surface motion year. There is also year-on-year variation in seasonal amplitude, likely to be related to interannual variation in the local water table coupled with the amount of available unfilled pore space in the uppermost layer of the peat. In this sequence the polygon sites indicate that the peatland became gradually more saturated, to the point that by 2017-2018 there were relatively fewer pores to fill, and annual surface motion
350 was reduced.

Synthesizing the above, the bimodal distribution of peatland surface motion timing within our landscape may be interpreted as reflecting two dominant components of the landscape, a drier shrub dominated and a wetter Sphagnum dominated component. Wetter, flatter sites in a 'near natural condition', typically dominated by SPH PFT tend to reach peak surface heights later in the year, have higher amplitudes and stable-positive velocities. Drier SHRUB and GRASS PFT dominated
355 sites tend to reach peak surface heights earlier in the year, have lower amplitude oscillations and negative velocities. That the distribution of surface motion metrics in this particular blanket bog landscape is bimodal reflects a combination of the natural state of the peatland and the legacy of past management.

3.3 Application to large area condition mapping

The observed relationship between surface motion metrics and ecohydrology is readily interpreted in the context of reported
360 field measurements of peat surface motion (Howie and Hebda, 2018; Morton and Heinemeyer, 2019). Flatter sites under near natural conditions are poorly drained, wetter and dominated by Sphagnum spp. In turn, Sphagnum spp have a considerable capacity for water storage as a direct result of their physiology (Kellner and Halldin, 2002), resulting in peak water storage and seasonal swelling of the surface late in the year. Drier sites with compacted peat have less capacity to store water and reach water holding capacity earlier in the autumn (Price, 2003). Furthermore, the more degraded peat in these
365 sites is less elastic and therefore exhibits a lower amplitude response to changes in water storage (Holden et al., 2004; Lui and Lennartz, 2019). As the seasonal water balance shifts, drier, better drained sites lose water first followed by the



Sphagnum sites which may continue to swell on account of a hysteresis during the first stages of water loss (Howie and Hebda, 2018).

370 With this interpretation of the relationship between the surface motion metrics and ecohydrology, it should be possible to use
the InSAR time series to map peatland condition. To illustrate this approach and evaluate its potential, a classified condition
map was generated (Fig. 4a). This map was based on the classified Euclidian distance (Materials and Methods) from an ideal
'wet' Sphagnum-dominated reference point (positive velocity, high amplitude, late winter peak timing) within a plot of
amplitude vs. peak timing vs. multiannual velocity for the entire study area. The resulting histogram of Euclidian distance
(Materials and Methods) was split into three broad peatland classes (Fig. 4). A Sphagnum class characterized by winter
375 (December to February) peak timing, high amplitude, and stable to positive velocity). A shrub class characterized by distinct
autumn (August to October) peak timing with lower amplitude and negative velocities. A thin/modified peat class,
characterized by both low amplitudes, negative velocities, and peak timing dissimilar to either the 'Sphagnum' or 'shrub'
class. These thin/modified areas are expected to correspond with the most degraded and drained grass dominated sites or
sites under restoration that are in transition to either a Sphagnum or shrub dominated state.

380 To assess the predictive accuracy of the Sphagnum class we determined the proportion of 328 pool systems that coincided
with pixels of that class. Although wet areas in which Sphagnum is dominant do not necessarily contain pool systems, the
reverse is nearly always true, and in the study area pool systems provide a spatially distributed, abundant and easily
identifiable sample of this part of the peatland system. They also correspond to the part of peatland systems most
unequivocally associated with 'near-natural' ecohydrological condition. The shrub and thin/modified classes are more likely
385 to correspond with areas in between on sloping, degraded, forested and formerly forested peatland, some of which may have
been much wetter prior to drainage.

A single marker was positioned in each selected pool system and the accuracy of the method determined based on whether
this marker lies within 150 m of a correctly classified pixel. There is a need to tolerate a level of uncertainty as pool systems
often display complex geometry related to local hydrology (Goode, 1973; Lindsay, 2016) and the position of the marker
390 point could not take this into account. On this basis, identification of wet peat conditions around the pool systems is 97.9%
accurate. Detailed inspection of the remaining 2.1% (7/328) of pool systems that did not fall within our threshold reveals that
these pool systems all showed evidence of localized erosion or drainage causing degradation of their natural hydrology.
From this, we can deduce that our method is converging towards 100% accuracy in identifying Sphagnum dominated pool
systems in a near natural ecohydrological condition.

395 Inspection of our classification relative to other known features indicates that the thin/modified class corresponds to areas
under restoration, notably areas recently felled for forest to bog restoration, areas subject to intensive grazing, thin peat soils
on steeper higher ground and in valley bottoms (Fig. 4b,c). The abundance of the thin/ modified class is striking in the east
of the study area that corresponds to long-term historical usage of the land for agriculture and associated cutting of peat for
fuel (Andersen et al., 2018; Minasny et al., 2019).



400 Our classification also provides an overall measure of the state of this blanket bog landscape, to which future regional change, on account of climate change or restoration, may be compared. For example, within the area, our method identifies approximately 254 km² (27.3 % of the area) as wet Sphagnum dominated peat, 481 km² (51.7 %) as shrub dominated peat, 117 km² (12.8 %) as the thin/modified peat class with 78 km² (8.4 %) as irregular time series.

4 Discussion

405 Our most important finding is that surface motion metrics derived from APSIS InSAR time series enable almost continuous spatial and temporal characterization of peatland condition at large scales. That the SAR data can penetrate cloud cover, measures regular physical displacement of the surface, and captures a known dynamic behavior associated with peat resilience gives this approach a significant lead over the far more challenging effort to measure peatland condition from optical reflectance data. This is compounded by the fact that cool wet peatlands are often obscured by cloud (Minasny et al.,
410 2019).

The sensitivity and dynamic response of surface motion metrics to changes in the state of the peatland system should make the method ideally suited to monitoring and informing peatland management and restoration. Globally, large areas of northern peatland degraded by historic drainage, grazing and forestry are now under or targeted for restoration (Rocheftort et al., 2017). As a consequence, peatland conservation and restoration are increasingly perceived as critical tools in the fight
415 against global climate change (Leifeld and Menichetti, 2018; Amelung et al., 2020; Günther et al., 2020). Restoration strategies typically involve raising water levels to re-establish wet conditions. The expectation is that this will promote Sphagnum establishment, often a key measure of the success of an intervention (Rocheftort et al., 2017; Bellamy et al., 2012; Caporn et al., 2018; González and Rocheftort, 2019).

In the case of blanket bog landscapes, our finding of naturally drier shrub and wetter Sphagnum states raises the question as
420 to whether a linear strategy of increasing peat wetness is always an appropriate restoration target, or indeed if it is the only desirable outcome in all peatland settings. In this context, an APSIS InSAR-based assessment of the condition of a whole peatland can help guide restoration strategies by, firstly identifying the typical natural states and hydrological structure of that peatland, and secondly, following intervention, this approach could enable a robust monitoring of restoration trajectories and outcomes.

425 In natural landscapes, these peatland states are a consequence of landscape evolution in which the vertical accumulation of peat must be counterbalanced on an appropriate spatial and temporal scale by erosion (Large et al., 2021). Drier states correspond to areas of net carbon loss due to natural drainage, incision and erosion along peatland margins, and wetter states correspond to peatland interiors, areas with low gradient, that tend towards carbon accumulation. In this context to restore a site that is naturally dry to the wet state would risk instability, while the opposite would fail to optimize carbon storage. A
430 more suitable and sustainable ambition is to accept that restored blanket bog sites may follow different trajectories towards naturally Sphagnum or shrub states, and that these target end states will be constrained by the hydrological landscape setting,



as conceptualized by Winter (Winter, 1988). Our approach provides evidence for these natural states co-existing within the study areas, and evidence to guide and monitor appropriate restoration trajectories within this system. Recognizing and preserving this mosaic is critical in maintaining large- and small-scale peatland landscape stability and carbon balances, particularly as long-term models suggest that the natural drying out of peatland is accelerating due to drainage (Harris et al., 2020; Leifeld et al., 2019) and climate change (Gallego-Sala and Prentice, 2013).

The approach outlined here should be readily transferable to alternative peatland settings within different parts of the global peatland climate space. Using surface motion metrics identified from the InSAR time series of peatland motion, a surface deformation space for a given peatland system can be defined. The position of ecohydrological characteristics within this space can then be deployed to quantify the state of the peatland system and map changes with respect to climate change and management intervention. This capacity to customize the approach is valuable as it provides the means to measure peatland condition at a global scale. If realized, this would enhance our understanding of the large-scale functionality of peatland landscapes and provide the robust evidence base required for sustainable peatland management.

Data availability

doi: [10.17639/nott.7123](https://doi.org/10.17639/nott.7123)

Supplement Link

Supplement supplied

Author Contribution

A.S. led the processing of the InSAR data that A.V.B. post-processed, analyzed and visualized. R.A. recorded the polygon attributes, mapped the pools, contributed to data visualization and completed the ground surveys with C.M. D.J.L developed the overall idea of applying InSAR for this purpose. All authors were responsible for critical contributions, passing the final manuscript and editing text and figures.

Competing Interests

Andrew Sowter is affiliated with Terra Motion Limited. The APSIS (Advanced Pixel System using Intermittent SBAS) method is owned by the University of Nottingham and is the subject of a UK Patent Application (No. 1709525.8) with the inventor named as Dr. Andrew Sowter; it is currently Patent Pending.



Disclaimer

We are not responsible for the consequences of any decisions or actions even if they have been influenced by the material and ideas in this manuscript.

460 Acknowledgments

The authors would like to thank members of the following organizations who provided access to sites for surveys or insight and local knowledge about past and present management over the study area: NatureScot Peatland ACTION, Royal Society for the Protection of Birds, Plantlife Scotland, Forestry and Land Scotland, Scottish Forestry, Welbeck Estate and Shurrery Estate. David Gee and Ahmed Athab for their assistance with the APSIS InSAR data output. “National Soil Map of
465 Scotland” copyright and database right The James Hutton Institute v.1_4. Used with the permission of the James Hutton Institute. All rights reserved. Any public sector information contained in these data is licensed under the Open Government License v.2.0. R.A. and C.M are funded by a Leverhulme Leadership Award (1466NS) and D.J.L, R.A. and C.M. with a NERC InSAR TOPS NE/P014100/1.

References

- 470 Alshammari L., Large D.J., Boyd, D.S., Sowter S., Anderson R., Andersen R., and Marsh S.: Long-term peatland condition assessment via surface motion monitoring using the ISBAS DInSAR technique over the Flow Country, Scotland. *Remote Sens.*, 10, 1-24, doi:10.3390/rs10071103, 2018.
- Alshammari, L., Boyd, D.S., Sowter, A., Marshall, C., Andersen, R., Gilbert, P., Marsh, S., and Large, D.J.: Use of surface motion characteristics determined by InSAR to assess peatland condition, *J. Geo. Res: Biogeosciences*, 125,
475 e2018JG004953, doi:10.1029/2018JG004953, 2020.
- Andersen, R., Cowie, N., Payne, R.J., and Subke, J.A.: The Flow Country peatlands of Scotland. *Mires and Peat*, 23, 1-2, doi:10.19189/MaP.2018.OMB.381, 2018.
- Almendinger, J.C., Almendinger, J.E., and Glaser, P.H.: Topographic fluctuations in across a spring fen and raised bog in the Lost River Peatland, northern Minnesota. *J. Ecol.*, 74, 393-401, doi:10.2307/2260263, 1986.
- 480 Amelung, W., Bossio, D., de Vries, W., Kögel-Knabner, I., Lehmann, J., Amundson, R., Bol, R., Collins, C., Lal, R., Leifeld, J. and Minasny, B.: Towards a global-scale soil climate mitigation strategy, *Nat. Comms.*, 11(1), 1-10, doi:10.1038/s41467-020-18887-7, 2020.
- Baden, W., and Eggelsmann, R.: *Der Wasserkreislauf eines nordwestdeutschen Hochmoores*. Verlag Wasser und Boden, Hamburg, Germany, 1964.
- 485 Bateson, L., Cigna, F., Boon, D. and Sowter, A.: The application of the Intermittent SBAS (ISBAS) InSAR method to the South Wales Coalfield, UK. *Int. J. App. Earth Obs. Geoinform.*, 34, 249–257, doi:10.1016/j.jag.2014.08.018, 2015.



- Becker, R. A., Chambers, J. M., and Wilks, A. R.: The New S Language. Wadsworth & Brooks/Cole, 1988.
- Bellamy, P.E., Stephen, L., Maclean, I.S., and Grant, M.C.: Response of blanket bog vegetation to drain-blocking. *Appl. Veg. Sci.*, 15(1), pp.129-135, doi:10.1111/j.1654-109X.2011.01151.x, 2012.
- 490 Box, G.E.P. and Cox, D.R.: An Analysis of Transformations. *J. R. Stat. Soc. B Methodol.*, 26(2) 211-252 (1964).
- Buras, A., Rammig, A., and Zang, C.S.: Quantifying impacts of the 2018 drought on European ecosystems in comparison to 2003. *Biogeosciences*, 17(6), 1655-1672, doi:10.5194/bg-17-1655-2020, 2020.
- Caporn, S.J.M., Rosenburgh, A.E., Keightley, A.T., Hinde, S.L., Riggs, J.L., Buckler, M. and Wright, N.A.: Sphagnum restoration on degraded blanket and raised bogs in the UK using micropropagated source material: a review of progress. *Mires and Peat*, 20, 1-17, doi:10.19189/MaP.2017.OMB.306, 2018.
- 495 Chen, C.W., and Zebker, H.A.: Two-dimensional phase unwrapping with use of statistical models for cost functions in nonlinear optimization. *J. Opt. Soc. Am. A*, 18, 338–351, doi:10.1364/JOSAA.18.000338, 2001.
- Cigna, F., and Sowter, A.: The relationship between intermittent coherence and precision of ISBAS InSAR ground motion velocities: ERS-1/2 case studies in the UK. *Remote Sens. Environ.*, 202, 177–198, doi:10.1016/j.rse.2017.05.016, 2017.
- 500 Crump J. (Ed.), *Smoke on water: Countering global threats from peatland loss and degradation*. UNEP, GRIDA, GPI, 2017.
- S.Fiaschi, E.P. Holohan, M. Sheehy, M. Floris, PS-InSAR Analysis of Sentinel-1 Data for Detecting Ground Motion in Temperate Oceanic Climate Zones: A Case Study in the Republic of Ireland. *Remote Sens.*, 11(3), doi:10.3390/rs11030348, 2019.
- Fritz, C., Campbell, D.I., and Schipper, L.A.: Oscillating peat surface levels in a restiad peatland, New Zealand – magnitude and spatiotemporal variability. *Hydrol. Processes*. 22, 3264-3274 doi: 10.1002/hyp.6912, 2008.
- 505 Glaser P.H., Chanton J.P., Morin P., Rosenberry D.O., Siegel D.I., Ruud O., Chasar L.I., and Reeve A.S.: Surface deformations as indicators of deep ebullition fluxes in a large northern peatland. *Global Biogeochem. Cycles* 18, GB1003, doi:10.1029/2002GB002069, 2004.
- Gallego-Sala, A.V., and Prentice, I.C.: Blanket peat biome endangered by climate change. *Nat. Clim. Change*. 3(2), 152-155, doi:10.1038/nclimate1672, 2013.
- 510 Ghil M., Allen M. R., Dettinger M. D., Ide K., Kondrashov D., Mann M. E., Robertson A. W., Saunders A., Tian Y., Varadi F., and Yiou P.: Advanced spectral methods for climatic time series. *Rev. Geophys.* 40, 1-40, doi:10.1029/2000RG000092, 2002.
- Gong, W., Thiele, A., Hinz, S., Meyer, F.J., Hooper, and A., Agram, P.S.: Comparison of small baseline interferometric SAR processors for estimating ground deformation. *Remote Sens.* 8, 330, doi:10.3390/rs8040330, 2016.
- 515 González, E., and Rochefort, L.: Declaring success in Sphagnum peatland restoration: Identifying outcomes from readily measurable vegetation descriptors. *Mires and Peat*. 24(19), 1-16, doi:10.19189/MaP.2017.OMB.305, 2019.
- Goode, D.A.: The significance of physical hydrology in the morphological classification of mires. *Classification of Peat and Peatlands*. In *Proc Int. Peat Soc. Symp.*, Eds. International Peat Society, Glasgow. pp10–20, 1973.



- 520 Günther, A., Barthelmes, A., Huth, V., Joosten, H., Jurasinski, G., Koebisch, F. and Couwenberg, J.: Prompt rewetting of drained peatlands reduces climate warming despite methane emissions, *Nat. Comms.*, 11(1), 1-5, doi:10.1038/s41467-020-15499-z, 2020.
- Hancock, M.H., England, B., and Cowie, N.R.: Knockfin Heights: a high-altitude Flow Country peatland showing extensive erosion of uncertain origin. *Mires & Peat*. 23, 1-20, doi:10.19189/MaP.2018.OMB.334, 2018.
- 525 Harris, L.I., Roulet, N.T., and Moore, T.R.: Drainage reduces the resilience of a boreal peatland. *Environ. Res. Commun.* 2(6), p.065001, doi:10.1088/2515-7620/ab9895, 2020.
- Holden, J., Chapman, P.J., and Labadz, J.C., Artificial drainage of peatlands: hydrological and hydrochemical process and wetland restoration. *Prog. Phys. Geogr.* 28, 95–123, doi:10.1191/0309133304pp403ra, 2004.
- Howie, S.A., and Hebda, R.J.: Bog surface oscillation (mire breathing) a useful measure in raised bog restoration. *Hydrol. Process.*, doi: 10.1002/hyp.11622, 2018.
- 530 Hutchinson, J. N.: The record of peat wastage in the East Anglian fenlands at Holme Post, 1848-1978 A.D. *J. Ecol.*, 68, 229-249, 1980.
- Hyndman, R., Athanasopoulos, G., Bergmeir, C., Caceres, G., Chhay, L., O’Hara-Wild, M., Petropoulos, F., Razbash, S., Wang, E. and Yasmeeen, F.: Forecast: Forecasting functions for time series and linear models. R package version 8.5. URL:<http://pkg.robjhyndman.com/forecast>, 2019.
- Jarvis, A., Reuter, H.I., Nelson, A., and Guevara, E.: Hole-filled seamless SRTM data V4, International Centre for Tropical Agriculture (CIAT), available at <http://srtm.csi.cgiar.org>, 2008.
- JHI, The James Hutton Institute, “National Soil Map of Scotland” available at <https://www.hutton.ac.uk/learning/natural-resource-datasets/soilshutton/soils-maps-scotland>. Last accessed 01 June 2021.
- 540 Kellner, E., and Halldin, S.: Water budget and surface-layer water storage in a Sphagnum bog in central Sweden. *Hydrol. Process.*, 16(1), 87-103, doi:10.1002/hyp.286, 2002.
- Kennedy, G.W., and Price, J.S.: A conceptual model of volume-change controls in the hydrology of cutover peats. *J. Hydrol.*, 302, 13-25, doi:10.1016/j.hydrol.2004.06.024, 2005.
- Kulczynski, S., Peat bogs of Polsie. *Memoires de l’Academie Polenaise des Sciences et des Lettres. Class de Sciences Mathematiques et Naturelles. Serie B: Sciences Naturelles.* 15, 1949.
- 545 Kurimo, H.: Surface fluctuation in three virgin pine mires in eastern Finland. *Silva Fennica*, 17, 45-64, 1983.
- Large, D.J., Marshall, C., Jochmann, M., Jensen, M., Spiro, B.F. and Olausson, S.: Time, Hydrologic Landscape, and the Long-Term Storage of Peatland Carbon in Sedimentary Basins. *J. Geo. Res.: Earth. Surf.*, 126(3) doi:10.1002/essoar.10503762.1, 2021.
- 550 Lees, K.J., Quaipe, T., Artz, R.E.E., Khomik, M., and Clark, J.M.: Potential for using remote sensing to estimate carbon fluxes across Northern peatlands: a review. *Sci. Tot. Env.*, 615, 857874, doi:10.1016/j.scitotenv.2017.09.103, 2018.



- Leifeld, J., and Menichetti, L.: The underappreciated potential of peatlands in global climate change mitigation strategies. *Nat. Commun.*, 9(1), 1-7, doi:10.1038/s41467-018-03406-6, 2018.
- Leifeld, J., Wüst-Galley, C., and Page, S.: Intact and managed peatland soils as a source and sink of GHGs from 1850 to 555 2100. *Nat. Clim. Change.*, 9(12), 945-947, doi:10.1038/s41558-019-0615-5, 2019.
- Liu, H., and Lennartz, B.: Hydraulic properties of peat soils along a bulk density gradient—A meta study. *Hydrol. Process.*, 33(1), 101-114, doi:10.1002/hyp.13314, 2019.
- Lindsay, R., Charman, D.J., Everingham, F., O'reilly, R.M., Palmer, M.A., Rowell, T.A. and Stroud, D.A.: The flow country: the peatlands of Caithness and Sutherland. D.A. Ratcliffe and P.H. Oswald Eds. (Nature Conservancy Council, Peterborough 560 1988), pp174. Available from Joint Nature Conservation Committee (JNCC) via <http://jncc.defra.gov.uk/page-4281>, 1988.
- Lindsay, R.: Peatland Classification. In: Everard, M., Finlayson, C.M., Irvine, K., McInnes, R.J., Middleton, B.A., Davidson, N.C. (Eds.) *The Wetland Book: I: Structure and Function, Management, and Methods*. Springer Nature, Netherlands, pp.1–14., 2018.
- Minasny, B., Berglund, Ö., Connolly, J., Hedley, C., Vries, F. D., Gimona, A., Kempen, B., Kidd, D., Lilja, H., Malone, B., 565 McBratney, A., Roudier, P., O'Rourke, S., Rudiyanto, Padarian, J., Poggio, L., Caten, A. T., Thompson, D., Tuve, C., and Widyatmanti, W.: Digital mapping of peatlands—A critical review. *Earth Sci. Rev.*, 196, 102870, doi:10.1016/j.earscirev.2019.05.014, 2019.
- Money, R.P., and Wheeler, B. D.: Some critical questions concerning the restorability of damaged raised bogs. *Appl. Veg. Sci.*, 2(1), 107–116, doi:10.2307/1478887, 1999.
- 570 Morton, P.A., and Heinemeyer, A.: Bog breathing: the extent of peat shrinkage and expansion on blanket bogs in relation to water table, heather management and dominant vegetation and its implications for carbon stock assessments. *Wetl. Ecol. and Manag.*, 27, 467–482 doi.org/10.1007/s11273-019-09672-5, 2019.
- Mustonen, S.E., and Seuna, P.: Metsäojitusksen vaikutuksesta suon hydrologiaan. Pages 1-63 in Publication 2, National Board of Waters, Finland, Water Research Institute, 1971.
- 575 Osmanoğlu, B., Sunar, F., Wdowinski, S., and Cabral-Cano, E.: Time series analysis of InSAR data: methods and trends. *ISPRS J. Photogramm. Remote Sens.*, 115, 90–102, doi:10.1016/j.isprsjprs.2015.10.003, 2016.
- Poggio, L., and Gimona, A.: National scale 3D modelling of soil organic carbon stocks with uncertainty propagation—an example from Scotland. *Geoderma*, 232, 284-299, doi:10.1016/j.geoderma.2014.05.004, 2014.
- Price, J.S.: Role and character of seasonal peat soil deformation on the hydrology of undisturbed cutover peatlands. *Water 580 Resour. Res.*, 39(9) 1214, doi:10.1029/2002WR001302, 2003.
- Price, J.S., and Schlotzhauer, S.M.: Importance of shrinkage and compression in determining water storage changes in peat: the case of a mined peatland. *Hydrol. Process.*, 13 2591-2601, doi:10.1002/(SICI)1099-1085(199911)13:16<2591::AID-HYP933>3.0.CO;2-E, 1999.



- R Core Team, R: A language and environment for statistical computing. R Foundation for Statistical Computing, Vienna, Austria. Available at <http://www.R-project.org/>, 2013.
- R Core Team: 'Stats v3.6.2' R package, available at <https://www.rdocumentation.org/packages/stats>, 2020.
- Reeve, A.S., Glaser, P.H., and Rosenberry, D.O.: Seasonal changes in peatland surface elevation recorded at GPS stations in the Red Lake Peatlands, northern Minnesota, USA. *J. Geophys. Res.: Biogeosci.*, 118, 1616-1626, doi:10.1002/2013JG002404, 2013.
- 590 Rochefort, L., and Andersen, R.: Global Peatland Restoration after 30 years: where are we in this mossy world?. *Rest Ecol.*, 25(2), 269-270, doi:10.1111/rec.12417, 2017.
- Roulet, N.T., Surface level and water table fluctuations in a subarctic fen, *Arc. Alp. Res.*, 23 (3), 303-310, 1991.
- Sloan, T.J., Payne, R.J., Anderson, A.R., Bain, C., Chapman, S., Cowie, N., Gilbert, P., Lindsay, R., Mauquoy, D., Newton, A.J. and Andersen, R.: Peatland afforestation in the UK and consequences for carbon storage, *Mires and Peat*, 23, doi.org10.19189/MaP.2017.OMB.315, 2018.
- 595 SNH, available at <http://gateway.snh.gov.uk/natural-spaces/index.jsp> (last accessed 24/07/20), 2019.
- Sowter, A., Che Amat, M., Cigna, F., Marsh, S., Athab, A., and Almshammari, L.: Mexico City land subsidence in 2014-2015 with Sentinel-1 IW TOPS: Results using the Intermittent SBAS (ISBAS) technique. *Int. J. App. Earth Obs. Geo.*, 52, 230-242, doi:10.1016/j.jag.2016.06.015, 2016.
- 600 Sowter, A., Bateson, L., Strange, P., Ambrose, K., and Syafiudin, M.F.: DInSAR estimation of land motion using intermittent coherence with application to the South Derbyshire and Leicestershire coalfields. *Rem. Sens. Lett.*, 4(10), 979-987, doi:10.1080/2150704X.2013.823673, 2013.
- SPECTRA software: <http://research.atmos.ucla.edu/tcd/ssa/guide/guide4.html>, last accessed 2 May 2021
- Tampuu, T., Praks, J., Uiboupin, R., and Kull, A.: Long Term Interferometric Temporal Coherence and DInSAR Phase in Northern Peatlands. *Rem. Sens.*, 12(10), 1566, doi: 10.3390/rs12101566, 2020.
- 605 Waddington, J.M., Morris, P.J., Kettridge, N., Granath, G., Thompson, D.K. and Moore, P.A.: Hydrological feedbacks in northern peatlands. *Ecohydrol.*, doi:10.1002/eco.14938(1), 113-127, 2015.
- Waddington, J.M., Kellner, E., Strack, M., and Price, J.S.: Differential peat formation, compressibility, and water storage between peatland microforms: Implications for ecosystem function and development. *Wat. Res. Res.* 46, W07538, doi:10.1029/2009WR008802, 2010.
- 610 Winter, T.C.: A conceptual framework for assessing cumulative impacts on the hydrology of nontidal wetlands. *Env. Man.*, 12(5), 605-620, doi:10.1007/BF01867539, 1988.